

Numerical study of long-term settlement following twin tunnel construction

Estudio numérico de asentamientos de largo plazo debido a la construcción de túneles gemelos

Fecha de envío: 6 de enero 2015

Fecha de aceptación: 29 de abril 2015

Rafael Martínez¹, Felix Schroeder² and David Potts³

¹ Constructora Lancuyen, Cochrane 635, piso 15, of. 1503, torre A, Concepción, Chile, rmartinez@lancuyen.cl

² Geotechnical Consulting Group, 52A Cromwell Road, London SW7 5BE, United Kingdom, f.c.schroeder@gcg.co.uk

³ Department of Civil and Environmental Engineering, Imperial College London, South Kensington Campus, London SW7 2AZ, United Kingdom, d.potts@imperial.ac.uk

This article presents a parametric study that uses the finite element (FE) method to analyse the problem of long-term settlements following twin tunnel construction in low permeability clay. Similar ground conditions to those typically found in central London, UK, were modelled. The construction process of the tunnels was simulated and thereafter a special boundary condition was used, enabling the FE model to consider the tunnels as fully permeable drains during the post-construction period. Several tunnel depths and separations were studied. The long-term interaction between the tunnels and the manner in which the long-term displacements - both vertical and horizontal - developed, were analysed. Conclusions are drawn about the principal factors that drive these movements. Finally, the potential building damage associated with the short and long-term movements obtained from the FE analyses is assessed, compared and discussed.

Este artículo presenta un estudio paramétrico que usa el método de elementos finitos para analizar el problema de asentamientos a largo plazo producto de la construcción de túneles gemelos en una arcilla de baja permeabilidad. Se modelaron condiciones del suelo similares a las encontradas en el centro de Londres, Reino Unido. El proceso de construcción de los túneles fue modelado y luego se utilizó una condición de borde especial que permitió considerar los túneles como drenes completamente permeables para el periodo posterior a la construcción. Se estudiaron distintas configuraciones de profundidad y separación de los túneles. Se analizó la interacción a largo plazo entre los túneles y también la forma en que se desarrollan los desplazamientos verticales y horizontales. Se concluyó respecto a los principales factores que afectan estos movimientos. Finalmente, se evalúa, compara y discute el potencial daño a las estructuras debido a los movimientos de corto y largo plazo generados por los túneles.

Keywords: twin tunnels, long-term settlement, clay, finite element, building damage

Palabras clave: túneles gemelos, asentamiento a largo plazo, arcilla, elementos finitos, daño a estructuras

Introduction

The fact that settlements continue to increase for a number of years following construction of tunnels in clayey soils has been recognised for many years. One of the reasons for these post-construction, or long-term, movements is that tunnels act as drains and reduce pore water pressures in the surrounding clay, thereby increasing the effective stress and causing consolidation to occur. Evidence from recent projects in the London area, most notably the Jubilee Line Extension (JLE), has shown that long-term

settlement occurs consistently in a wide range of urban and greenfield situations. However, the magnitude and rate of the consolidation induced settlements varies greatly. Generally, long-term movements occur over a much wider area than the immediate (short-term) movements which occur during construction. This means that when assessing the impact of tunnels on overlying infrastructure (e.g. buildings) additional assets may require consideration under long-term conditions as compared to the short-term conditions.

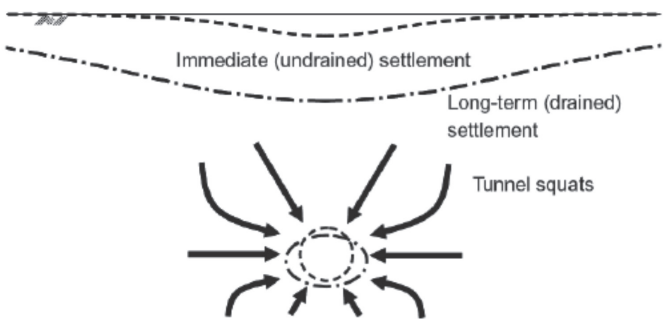


Figure 1: Tunnel in clay acting as long-term drain (Mair, 2008)

As illustrated schematically in Figure 1, the long-term settlement trough has been reported to be deeper and wider than the short-term one (e.g. Mair and Taylor, 1997; Burland *et al.*, 2001). New and O'Reilly (1991) considered measured settlements above a 3.0 m diameter tunnel in Grimsby, UK, 7 days and 11 years after tunnel construction. They concluded that the effects of deepening of the settlement trough were largely mitigated by its widening in that the angular distortions at the surface ground were not considerably altered. In their discussion, they added that the maximum horizontal strains induced by the consolidation process would not be expected to exceed those present after 7 days. New and O'Reilly (1991) also report on measured pore water pressures in the ground surrounding the tunnel and found no evidence of reduced pore pressures, even within a few meters of the tunnel. This is in contrast to measurements presented by Mair (2008) which show significant pore pressure reductions in the vicinity of London Underground tunnels at a number of locations across the London tube network, indicating that tunnels frequently act as drains, particularly when located in low permeability soils, such as the London Clay.

This article presents a parametric study that uses the finite element (FE) method to analyse the problem of long-term settlements following twin tunnel construction in low permeability clay. Due to the extensive tunnelling activity in London over recent decades, including the Jubilee Line Extension and more recently Crossrail, similar ground conditions to those found in central London were modelled.

Soil properties and problem setup

The present study was carried out using the FE program ICFEP (see Potts and Zdravkovic, 1999 and 2001). The

parametric study presented herein considers two circular tunnels with a diameter of 4.75 m located at the same level below the ground surface. The parameters varied were the tunnel depth, D , and the separation, S , between them (see Figure 2). The range of geometries considered is presented in Table 1.

Table 1 Geometries analysed

| Run | X (horizontal) - Coordinate* | | separation | | tunnel axis depth (m)** |
|-------|------------------------------|-------------------|------------|----------------------|-------------------------|
| | left tunnel axis | right tunnel axis | meters | multiple of Diameter | |
| Run 1 | 125 | 147 | 22 | 5D | 29 |
| Run 2 | 125 | 147 | 22 | 5D | 17 |
| Run 3 | 125 | 147 | 22 | 5D | 41 |
| Run 4 | 100 | 172 | 72 | 15D | 41 |
| Run 5 | 100 | 172 | 72 | 15D | 29 |
| Run 6 | 100 | 172 | 72 | 15D | 17 |
| Run 7 | 112 | 160 | 48 | 10D | 41 |
| Run 8 | 112 | 160 | 48 | 10D | 29 |
| Run 9 | 112 | 160 | 48 | 10D | 17 |
| Run10 | 125 | - | Infinite | Infinite | 41 |
| Run11 | 125 | - | Infinite | Infinite | 29 |
| Run12 | 125 | - | Infinite | Infinite | 17 |

Tunnel diameter = 4.75m * X-coordinate measured to the right from upper right FE mesh corner
** Depth measured downwards from upper horizontal FE mesh boundary

Other parameters, such as the soil properties and all of the boundary conditions remained the same for all the analyses. The stratigraphy adopted for all analyses is typical for central London and is presented in Figure 3. Figure 3 also presents the initial pore water pressure distribution assumed showing the under-drained profile characteristic for many parts of London.

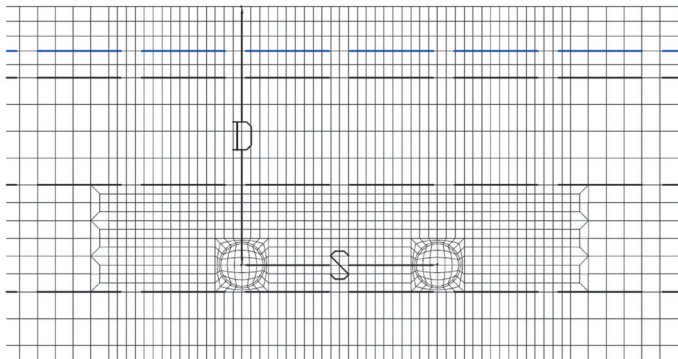


Figure 2: Tunnel separation S and tunnel depth D

An extract of the FE mesh developed for one of the analyses is shown in Figure 2. The width of the overall mesh for all analyses was 272 m and the depth 68 m. This ensures that for the maximum tunnel separation considered ($S = 15D$ or 72 m) there is a minimum distance of 100 m between each tunnel axis and the closest vertical mesh boundary (with no horizontal movements allowed). For the lower horizontal boundary neither vertical nor

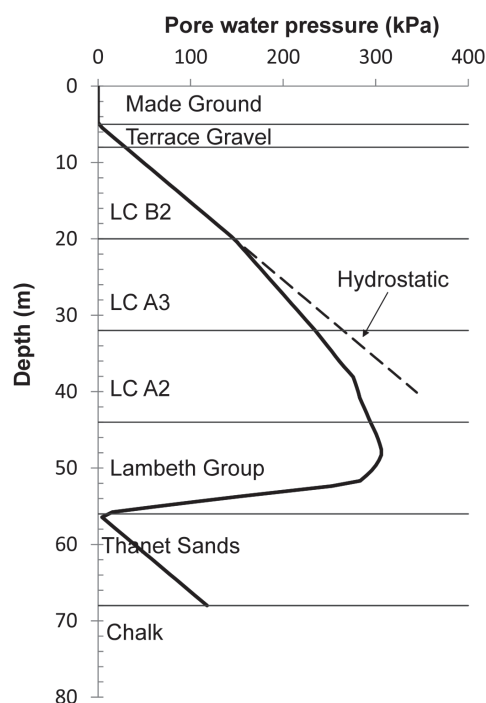


Figure 3: Stratigraphy and pore water pressure profile adopted for the analyses

horizontal movements were allowed. 8-node plane-strain isoparametric quadrilateral elements were used to model the soil and 3-node beam elements (Day and Potts, 1990) were used to model the tunnels' concrete lining. The segmental nature of the linings was not explicitly modelled, as the stresses acting in the linings were not expected to exceed the capacity of the joints between individual segments. A coupled consolidation formulation was used and an accelerated modified Newton-Raphson scheme with sub-stepping stress point algorithm was employed to solve the non-linear finite element equations. The stratigraphy considered in the study has Chalk at a depth of 68 m below ground surface. This stratum is significantly stiffer and stronger than the overlying materials and therefore, the bottom mesh boundary (with no horizontal and vertical movements allowed) was placed at the top of the Chalk.

The construction sequence adopted in all analyses is given in Table 2. The initial under-drained pore water pressure profile shown in Figure 3 has to be in equilibrium with the assumed permeability distribution and the hydraulic boundary conditions. While the input was chosen to closely approximate the correct pore pressure profile, a long time period was allowed at the beginning of the analysis (increments 1 to 5) to ensure full equilibrium.

However, the stress and displacement changes during this period were very small and any results presented in this paper do not include changes during the first 5 increments.

Table 2: Construction sequence

| Increment | Time | Activity |
|-----------|------------|-------------------------------|
| 1-5 | 1000 years | Stabilisation period |
| 6-25 | 7 days | 1st (left) tunnel excavation |
| 26-30 | 7 days | Rest period |
| 31-50 | 7 days | 2nd (right) tunnel excavation |
| 51-70 | 180 years | Consolidation |

Tunnel construction was modelled using a full face 'convergence-confinement' method (Potts and Zdravkovic, 2001) targeting a volume loss $V_L = 1.5\%$ for the first tunnel. For the construction of the second tunnel, the same percentage of unloading was assumed prior to the construction of the tunnel lining. This results in a larger volume loss for the second tunnel and takes account of the fact that this tunnel would not have been built under greenfield conditions but assumes that a similar construction method would have been used for both tunnels.

Hydraulic boundary conditions

Made Ground, Terrace Gravels and Thanet Sands are all granular materials which were allowed to drain freely without changes in pore pressure throughout the analyses. The London Clay (LC) units (B2, A3 and A2) and the Lambeth Group were considered to be consolidating materials using the log law permeability model proposed by Vaughan (1989). In this model the permeability k is defined as $k = k_0 e^{-Bp'}$, where k_0 is the permeability at zero mean effective stress, p' is the mean effective stress and B is a material property. In order to obtain the under-drained pore water pressure profile shown in Figure 3, $B = 0.007$ was chosen. The k_0 adopted for all the consolidating materials was $k_0 = 2.0 \cdot 10^{-9}$ m/s. The tunnels were considered to act as drains and a special boundary condition that ensures that the tunnels do not act as sources of water when suctions are detected at the tunnel boundary was used. This boundary condition only allows water to flow into the tunnels when compressive pore water pressures are detected at this boundary. This special boundary condition was activated for each tunnel after the completion of their construction.

Material properties

The Made Ground was modelled as an isotropic linear elastic perfectly plastic material with a drained Young's Modulus $E' = 10000$ kPa and an effective Poisson's ratio $\nu' = 0.2$. All the other strata were modelled as isotropic non-linear elastic perfectly plastic materials. The non-linear elastic model employed was based on that described by Jardine *et al.* (1986) with the parameters summarised in Table 3 and Table 4.

The perfect plasticity was modelled using a non-associated Mohr-Coulomb model. The yield surface is defined by the

strength parameters cohesion c' , and angle of shearing resistance ϕ' , and the plastic potential is defined by an angle of dilation ψ' . These parameters and the unit weights are given in Table 5 for all materials. For the post-construction consolidation period ψ' was assumed to be equal to zero.

The tunnel lining was modelled as a continuous elastic ring with the following parameters: bulk unit weight $\gamma = 24$ kN/m³, Young's modulus $E = 2.80 \cdot 10^7$ kN/m², Poisson's ratio $\nu = 0.15$, cross sectional area $A = 2.60$ m², second moment of area $I = 3.95 \cdot 10^{-4}$ m⁴/m, *i.e.* a lining thickness of $t = 0.168$ m.

Table 3: Coefficients and limits for non-linear elastic shear modulus

| Stratum | A | B | C , % | β | γ | $E_{d,min}$, % | $E_{d,max}$, % | G_{min} , kPa |
|-----------------------|------|------|---------|---------|----------|-----------------|-----------------|-----------------|
| Terrace Gravel | 1600 | 1550 | 0.0001 | 1.2 | 0.617 | 0.00346 | 0.69282 | 2333.3 |
| London Clay B2 | 702 | 827 | 0.0001 | 1.1 | 0.617 | 0.0052 | 0.3 | 2000.0 |
| London Clay A3 | 702 | 827 | 0.0001 | 1.1 | 0.617 | 0.0052 | 0.3 | 2000.0 |
| London Clay A2 | 767 | 903 | 0.0001 | 1.1 | 0.617 | 0.0017 | 0.3 | 2000.0 |
| Lambeth Group (Clays) | 987 | 875 | 0.0001 | 1.1 | 0.850 | 0.0025 | 0.3 | 2000.0 |
| Thanet Sands | 1200 | 1100 | 1.0E-04 | 1.3 | 0.617 | 0.0017 | 0.3 | 2000.0 |

Table 4: Coefficients and limits for non-linear elastic bulk modulus

| Stratum | R | S | T , % | δ | μ | $\varepsilon_{v,min}$, % | $\varepsilon_{v,max}$, % | K_{min} , kPa |
|-----------------------|-----|-----|---------------------|----------|-------|---------------------------|---------------------------|-----------------|
| Terrace Gravel | 600 | 580 | 0.001 | 1.90 | 0.42 | 0.005 | 0.15 | 3000 |
| London Clay B2 | 404 | 404 | 0.00035 | 1.81 | 0.34 | 0.001 | 0.2 | 2500 |
| London Clay A3 | 404 | 404 | 0.00035 | 1.81 | 0.34 | 0.001 | 0.2 | 2500 |
| London Clay A2 | 404 | 404 | 0.00035 | 1.81 | 0.34 | 0.001 | 0.2 | 2500 |
| Lambeth Group (clays) | 404 | 404 | 0.00035 | 1.81 | 0.34 | 0.001 | 0.3 | 2500 |
| Thanet Sands | 265 | 850 | $3.5 \cdot 10^{-4}$ | 1.20 | 0.34 | $3 \cdot 10^{-3}$ | 0.4 | 2500 |

Table 5: Mohr-Coulomb yield surface parameters, plastic potential parameters and unit weight.

| | MG | TG | LC (B2, A3, A2) | LG | TS |
|-------------------------------------|------|------|-----------------|----|-----|
| c' , kN/m ² | 0.0 | 0.0 | 5.0 | 10 | 0.0 |
| ϕ' , ° | 25.0 | 35.0 | 25.0 | 28 | 36 |
| ψ' , ° | 12.5 | 17.5 | 12.5 | 14 | 18 |
| Bulk unit weight, kN/m ³ | 18.0 | 20.0 | 20.0 | 20 | 20 |

Results and discussions

Figure 4 depicts the long-term settlement troughs for Runs 1 to 9 clearly illustrating the influence of the tunnels' separation, S , and their depth, D . In addition, Table 6 summarises the maximum surface settlement obtained at the end of construction of the second tunnel (short-term) and at the end of the consolidation process (long-term) for all the analyses. When comparing the maximum settlements obtained for the different analyses it can be seen that for a given tunnel separation S , the maximum long-term settlement is always obtained for a tunnel depth of 29 m, *i.e.* the intermediate depth considered in the study. At this depth the overall decrease in pore water pressure is a maximum, thus increasing the effective stresses and causing the long-term settlements. On the other hand the smallest maximum long-term settlement for a given tunnel separation is not always obtained for the same tunnel depth. For the single tunnel scenario the smallest maximum long-term settlement is obtained for the largest tunnel depth (Run 10 – $S = \text{Infinite}$, $D = 41$ m). This can be expected as for the deepest tunnel the reductions of pore water pressures associated with the tunnel acting as a drain spread over a wide area and hence result in relatively small settlements. This is also true for the largest separation of $S = 15D$ where there are two distinct peak in surface settlement for all tunnel depths (see Figure 4) and the smallest long-term settlement is obtained for the deepest tunnel. However, for $S = 10D$ the deepest tunnel scenario results in a single long-term settlement trough with a larger maximum settlement than for the shallowest scenario for which two distinct peaks remain. For $S = 5D$, a single long-term settlement trough is obtained for all tunnel depths, with the shallowest configuration giving the lowest maximum long-term settlement.

Figure 5 presents the pore water pressure distributions for profiles at different offsets X , from the vertical mesh boundary for the analyses with $S = 5D$. Profiles at $X = 125$ m are at approximately the left hand side tunnel axis, while the profiles at $X = 120$ m are around 2 m from the tunnel extrados. Also shown in Figure 5 is the free field pore water pressure distribution. This figure illustrates how the depth of the tunnels determines the pore pressure changes and thus the long-term surface settlements. It can be seen that the maximum overall pore pressure changes

are obtained for the tunnels at the intermediate depth of 29 m and hence explain the maximum long-term surface settlement obtained for this tunnel depth, as discussed above.

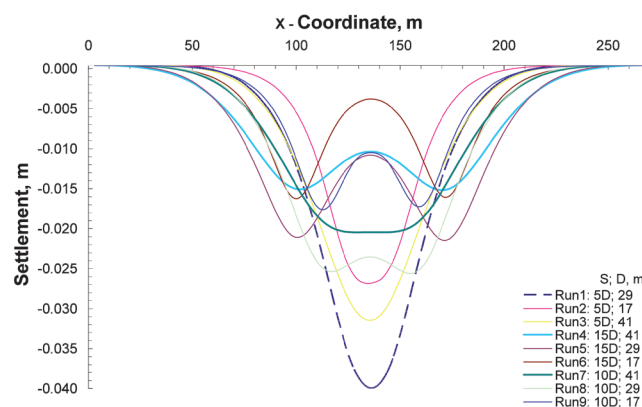


Figure 4: Long-term settlement trough comparison. Run 1 to 9

Table 6: Maximum surface settlement

| Run | Separation D ; Depth, m | Maximum settlement, mm | | Long/short - term ratio | min value max. value |
|-------|------------------------------|------------------------|-----------|----------------------------|-------------------------|
| | | Short-term | Long-term | | |
| Run 3 | 5D ; 41 | -9 | -32 | 3.45 | |
| Run 1 | 5D ; 29 | -7 | -40 | 6.13 | |
| Run 2 | 5D ; 17 | -12 | -27 | 2.31 | |
| Run 7 | 10D ; 41 | -6 | -21 | 3.77 | |
| Run 8 | 10D ; 29 | -7 | -26 | 3.92 | |
| Run 9 | 10D ; 17 | -9 | -18 | 1.96 | |
| Run 4 | 15D ; 41 | -5 | -16 | 3.38 | |
| Run 5 | 15D ; 29 | -6 | -22 | 3.53 | |
| Run 6 | 15D ; 17 | -9 | -17 | 1.92 | |
| Run10 | infinite ; 41 | -4 | -15 | 3.86 | |
| Run11 | infinite ; 29 | -6 | -21 | 3.86 | |
| Run12 | infinite ; 17 | -8 | -17 | 2.03 | |

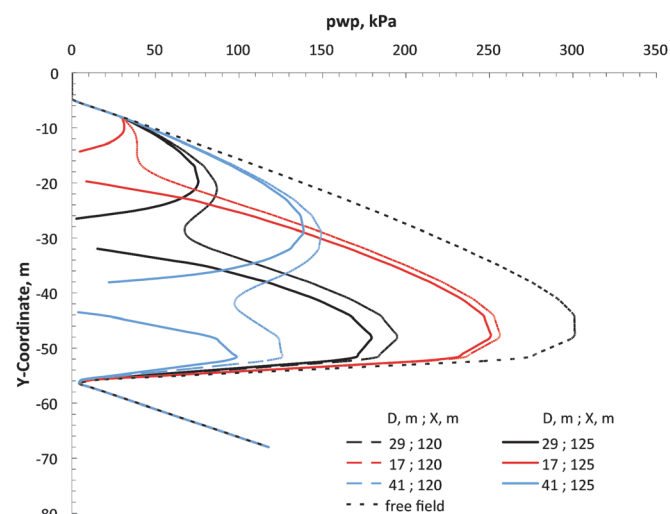


Figure 5: Pore water pressure profiles for $S = 5D$ different offsets X from the vertical mesh boundary

In order to assess the building damage potential for the different settlement troughs obtained from the FE analyses

the methodology proposed by Burland and Wroth (1974) was employed. For the long-term settlement trough for each analysis, a building length and location was determined to get the maximum deflection ratio Δ/L in hogging. For this building the deflection ratio Δ/L and maximum horizontal tensile strain ϵ_x were calculated for long-term and short-term conditions and plotted in an interaction diagram for the hogging mode (Burland, 1995). Figure 6 shows the results of these building damage analyses, with the black symbols representing long-term conditions and the grey symbols representing short-term conditions. It can be seen from Figure 6 that the long-term deflection ratio – horizontal strain combinations are always further away from the origin than their short-term equivalent. This implies that the potential long-term damage might be more significant than the short-term one. This result appears to be contrary to the findings of others (e.g. New and O'Reilly, 1991). It is important to note that, although the magnitude of the potential damage obtained from this parametric study is always low (Damage Category 0 or 1 according to the definition of Burland, 1995), the potential long-term damage is consistently higher than the corresponding short-term values. It should be remembered that in the present study, the magnitude of the potential damage parameters has been calculated assuming infinitely flexible buildings, which will be altered by the presence of the structures themselves (Potts and Addenbrooke, 1997). Furthermore, it may be that, although the potential damage in the long term are larger than in the short term, they are not as critical to building owners as they occur over extended periods of time (in some cases several decades),

during which routine maintenance, for example, may mask and/or alleviate some of the potential damage. In this manner, the results presented herein simply illustrate patterns of behaviour in terms of the effects of long-term settlement following tunnel construction that should be considered and may require detailed consideration.

Conclusions

Nine geometries for twin tunnels and 3 geometries for single tunnels were analysed using finite element models with a coupled consolidation approach to consider long-term post-construction settlements. It was observed that the magnitude of the settlements was driven by the overall effects of the tunnels, which were assumed to act as perfect drains, on the initial pore water pressure regime. It has been demonstrated that this overall drainage effect is a function of the tunnel configuration in terms of depth and separation. Other parameters that will have an influence, but were not considered herein are tunnel diameter, soil properties (especially permeability) and the initial pore water pressure profile. In this respect, the results presented in this study are specific for the conditions considered and further studies would be required to determine the effects of other parameters. The potential building damage as a result of short-term and long-term settlements were evaluated on the basis of the FE analysis results. It was found that the long-term damage consistently exceeds the short-term one, which is contrary to the view of some authors.

References

- Burland, J.B., Standing, J.R. and Jardine, F.M. (2001). Building response to tunnelling: case studies from construction of the Jubilee Line Extension, London. Volume 2: case studies, London, CIRIA and Thomas Telford
- Burland, J.B. (1995). Assessment of risk of damage to buildings due to tunnelling and excavation. *Proceedings 1st International Conference on Earthquake Geotechnical Engineering*, IS-Tokyo
- Burland, J.B. and Wroth, C.P. (1974). Settlement of buildings and associated damage. SOA Review. *Conf. Settlement of Structures*, Cambridge, Pentech Press, London, 611-654
- Day, R.A. and Potts, D.M. (1990). Curved Mindlin beam and axi-symmetric shell elements – A new approach. *International Journal for Numerical Methods in Engineering* 30, 1263-1274

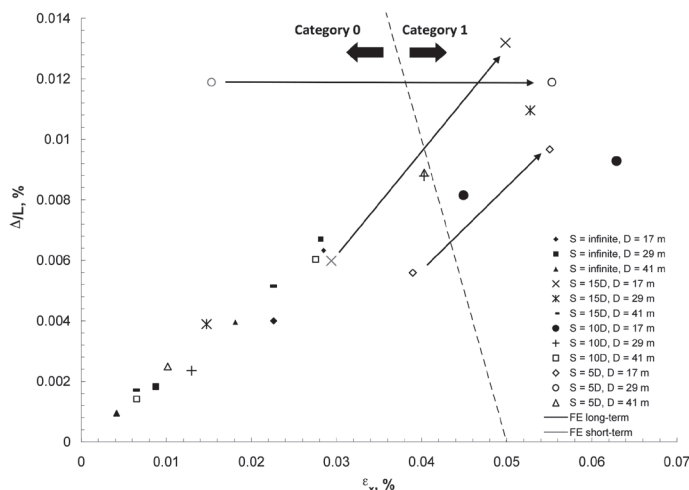
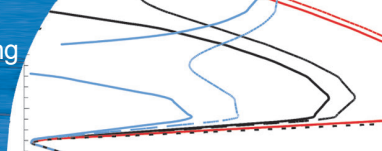


Figure 6: Short and long-term building damage assessment



- Jardine, R.J., Potts, D.M., Fourie, A.B. and Burland, J.B. (1986). Studies of the influence of non-linear stress-strain characteristics in soil-structure interaction. *Géotechnique* **36**, No. 3, 377-396
- Mair, R.J. (2008). Tunnelling and geotechnics: New horizons. *Géotechnique* **58**, No 9, 695-736
- Mair, R.J. and Taylor, R.N. (1997). Bored tunnelling in the urban environment: State-of-the-art report and theme lecture. *Proceedings 14th International Conference on Soil Mechanics and Foundation Engineering*, Hamburg **4**, 2353-2385
- New, B.M. and O'Reilly, M.P. (1991). Tunnelling induced ground movements: predicting their magnitude and effect. *Proceedings 4th International Conference on Ground Movements and Structures*, Cardiff, 671-697
- Potts, D.M. and Zdravkovic, L. (1999). *Finite element analysis in geotechnical engineering: Theory*. London: Thomas Telford
- Potts, D.M. and Zdravkovic, L. (2001). *Finite element analysis in geotechnical engineering: Application*. London: Thomas Telford.
- Potts, D.M. and Addenbrooke, T.I. (1997). A structure's influence on tunnelling-induced ground movements. *ICE Proceedings Geotechnical Engineering* **125**, N°2, 109-125
- Vaughan, P.R. (1989). Non-linearity in seepage problems: theory and field observations. *De Mello Volume*, 501-516, Sao Paulo: Editora Edgard Blucher Ltda.